Phosphorylation of hepatitis B virus Cp at Ser^{87} facilitates core assembly

Hee Yong KANG*, Seungkeun LEE*, Sung Gyoo PARK*†, Jaehoon YU‡, Youngsoo KIM§‖ and Guhung JUNG*[1]

*School of Biological Sciences, Seoul National University, Shillim-dong, Seoul 151-742, South Korea, †Institute of Microbiology, Seoul National University, Shillim-dong, Seoul 151-742, South Korea, ‡Department of Chemistry Education, Seoul National University, Shillim-dong, Seoul 151-742, South Korea, §Molecular Genomic Medicine, College of Medicine, Seoul National University, Yongon-dong, Seoul 110-799, South Korea, and ‖Cancer Research Institute, College of Medicine, Seoul National University, Yongon-dong, Seoul 110-799, South Korea

Protein–protein interactions can be regulated by protein modifications such as phosphorylation. Some of the phosphorylation sites (Ser^{155}, Ser^{162} and Ser^{170}) of HBV (hepatitis B virus) Cp have been discovered and these sites are implicated in the regulation of viral genome encapsidation, capsid localization and nucleocapsid maturation. In the present report, the dimeric form of HBV Cp was phosphorylated by PKA (protein kinase A), but not by protein kinase C *in vitro*, and the phosphorylation of dimeric Cp facilitated HBV core assembly. Matrix-assisted laser-desorption ionization–time-of-flight analysis revealed that the HBV Cp was phosphorylated at Ser^{87} by PKA. This was further confirmed using a mutant HBV Cp with S87G mutation. The S87G mutation inhibited the phosphorylation and, as a result, the *in vitro* HBV core assembly was not facilitated by PKA. In addition, when either pCMV/FLAG–Core(WT) or pCMV/FLAG–Core(S87G) was transfected into HepG2 cells, few mutant Cps (S87G) assembled into capsids compared with the wild-type (WT) Cps, although the same level of total Cps was expressed in both cases. In conclusion, PKA facilitates HBV core assembly through phosphorylation of the HBV Cp at Ser^{87}.

Key words: core protein (Cp), core assembly, hepatitis B virus (HBV), phosphorylation, protein kinase A (PKA).

INTRODUCTION

Human HBV (hepatitis B virus) is a member of the Hepadnaviridae family and has infected over two billion people worldwide [1]. Acute infections can result in serious illness, and chronic HBV infection causes liver diseases such as liver cirrhosis and hepatocellular carcinoma as well as other serious consequences [2]. HBV is currently classified into eight genotypes, A–H, on the basis of full-length genome sequencing. Variations in the viral infectivity and replication level are due to the genomic differences between the different genotypes [3–5].

HBV has a partially double-stranded DNA genome comprising four ORFs (open reading frames), denoted C, S, P, and X [6,7]. The C ORF encodes the HBV Cp (core protein), which plays an essential role in the life cycle of the virus. pgRNA (pregenomic RNA), HBV polymerase and other components such as heat shock proteins and protein kinases are packaged into the capsid, which is an assembled form of the Cp, and viral replication is able to commence.

HBV Cp is 183–185 amino acids long, consisting of an N-terminal assembly domain (amino acids 1–149) and a C-terminal protamine domain (amino acids 150–183 or 185) [8]. The N-terminal assembly domain is related to the HBV core assembly, while the C-terminal protamine domain is known for the regulation of viral replication [9]. The capsid comprises 90 ($T = 3$ form) or 120 ($T = 4$ form) Cp dimers [10]. The first step of HBV core assembly is the formation of dimeric forms of the Cp subunit from its monomers; a trimer of dimers then nucleates capsid assembly, followed by rapid addition of subsequent dimers [8]. Generally, Cp149, a 34-residue truncated form of the C-terminal domain of the HBV Cp, spontaneously forms a capsid under suitable conditions *in vitro* and *in vivo* [11,12]. This protein has been used for the study of core assembly because it can be overexpressed in *Escherichia coli* and is structurally similar to the HBV core antigen [10,13].

The process of HBV core assembly is related to the specific encapsidation of the pgRNA–polymerase complex mediated by HBV Cp phosphorylation [14,15]. Several kinases such as cdc2 kinase, PKA (protein kinase A), PKC (protein kinase C), 46 kDa serine kinase, SRPK1 (serine/arginine protein-specific kinase 1), and SRPK2 have been found to phosphorylate the HBV Cp [16–19]. The phosphorylation sites of the C-terminal protamine domain (Ser^{155}, Ser^{162}, and Ser^{170} in genotypes B, C, and D; Ser^{157}, Ser^{164}, and Ser^{172} in genotype A; and Thr^{239}, Ser^{245}, Ser^{257}, and Ser^{259} in duck hepatitis B virus) have been identified using these kinases and these sites were found to be related to the encapsidation of the pgRNA–polymerase complex, viral genome replication and capsid localization [14,18,20,21]. On the other hand, the roles and the sites of phosphorylation in the N-terminal assembly domain are unclear and only a cdc2 kinase-like recognition motif (Thr^{128}) has been identified [22].

In the present study, we observed that the PKA-mediated phosphorylation of HBV Cp at Ser^{87}, which is located in the N-terminal HBV Cp, facilitates the core assembly in the life cycle of HBV by increasing the affinity between HBV Cp dimers.

MATERIALS AND METHODS

Plasmids

A mutant Cp with S87G mutation was constructed using the forward primer 5′-TTAGTAGTCGGCTATGTCA-3′, the reverse primer 5′-TGACATAGCCGACTACTAA-3′ and pHBV1.2x as a template. The construct of pHBV1.2x genotype C was described previously [23]. The mutation was confirmed by nucleotide sequencing. To express the mutant Cp149(S87G) in *E. coli*, the

Abbreviations used: Cp, core protein; FC, flow cell; HBV, hepatitis B virus; MALDI–TOF, matrix-assisted laser-desorption ionization–time-of-flight; ORF, open reading frame; PKA, protein kinase A; PKC, protein kinase C; pgRNA, pregenomic RNA; RU, response unit; SPR, surface plasmon resonance; SRPK1, serine/arginine protein-specific kinase 1; TEM, transmission electron microscopy; WT, wild-type; WT PKA, PKA-treated wild-type.

[1] To whom correspondence should be addressed (email drjung@snu.ac.kr).

mutant Cp was constructed as described in [24]. The WT (wild-type) and mutant pCMV/FLAG–Core were constructed by fusing the FLAG-tag to pCMV-Core as described previously [23].

Cp149 protein expression and purification

The Cp149(S87G) mutant was cloned into the pET28b vector (Novagen, Madison, WI, U.S.A.) then transformed into BL21 (DE3) + pLysS *E. coli* (Novagen) and purified as described previously [24]. The assembly of mutant Cp149(S87G) was confirmed by native gel electrophoresis and Western blotting.

Detection of PKA-mediated core phosphorylation and assembly

For the experiments, 20 μM of purified dimeric Cp149 was incubated with reaction buffer (10 mM Hepes, pH 7.5 and 10 mM $MgCl_2$), 10 μM ATP and 1 unit of PKA (Sigma, St. Louis, MO, U.S.A.). For the inhibition experiment, serially diluted H-89 (1, 5 or 10 μM; PKA specific inhibitor; Sigma) was used. Samples were incubated at 30 °C for the designated times. After stopping the reaction with 50 mM EDTA, each sample was separated by electrophoresis on a 0.9 % native gel, followed by Western blot analysis with anti-HBc antibody (DAKO, Glostrup, Denmark) as described previously [23]. To detect the phosphorylation of Cp149, 10 μM of [γ-^{32}P]ATP (3000 Ci/mmol) was used instead of unlabelled ATP. PKC (1 unit; Promega, Madison, WI, U.S.A.) was used for the control experiment. The band intensities were analysed using ImageMaster 2D Elite software 4.01 (Amersham Pharmacia Biotechnology, Uppsala, Sweden).

Determination of binding affinity of proteins using SPR (surface plasmon resonance)

The analysis was performed using a BIAcore 3000 instrument (Biacore AB, Uppsala, Sweden). The samples (Cp149 treated with PKA or not treated) were denatured with 3.5 M urea and fractionated for the purification of Cp149 dimers as described previously [24]. FC1 (flow cell 1) was a negative control (without any proteins), while in the experimental flow cells, WT (FC2) and PKA-treated WT dimeric Cp149 (FC3) were immobilized according to the manufacturer's instructions. Results, measured as RUs (response units) were obtained with change of sensorgrams from FC2 and FC3 compared with FC1 for 100 s to detect the association rate or for 150 s to detect the dissociation rate. The temperature of the flow cell was maintained at 30 °C. To determine the binding affinity of immobilized Cp149, five concentrations of Cp149 dimer (10, 5, 2.5, 1.25, and 0.625 μM) were injected over the biosensor surface at a flow rate of 60 μl/min and the sensor chip was regenerated with 50 mM NaOH. Data were analysed with the BIAevaluation software version 3.1 (Biacore AB).

Electron microscopy and sucrose step gradient analysis

In vitro Cp149 assembly by PKA was performed as described above. Electron microscopy and sucrose step gradient analysis were carried out as described previously [24], except for the composition of the buffer (10 mM Hepes, pH 7.5 and 10 mM $MgCl_2$).

Detection of cytoplasmic HBV capsid in transfected cells

HepG2 cells were maintained in Dulbecco's modified Eagle's medium (Sigma) with 10 % (v/v) foetal bovine serum (GIBCO®, Grand Island, NY, U.S.A.). Cells were seeded in 100 mm diameter dishes and were transfected the following day with the appropriate DNA and FuGENE™ 6 (Roche) as described by the manufacturer.

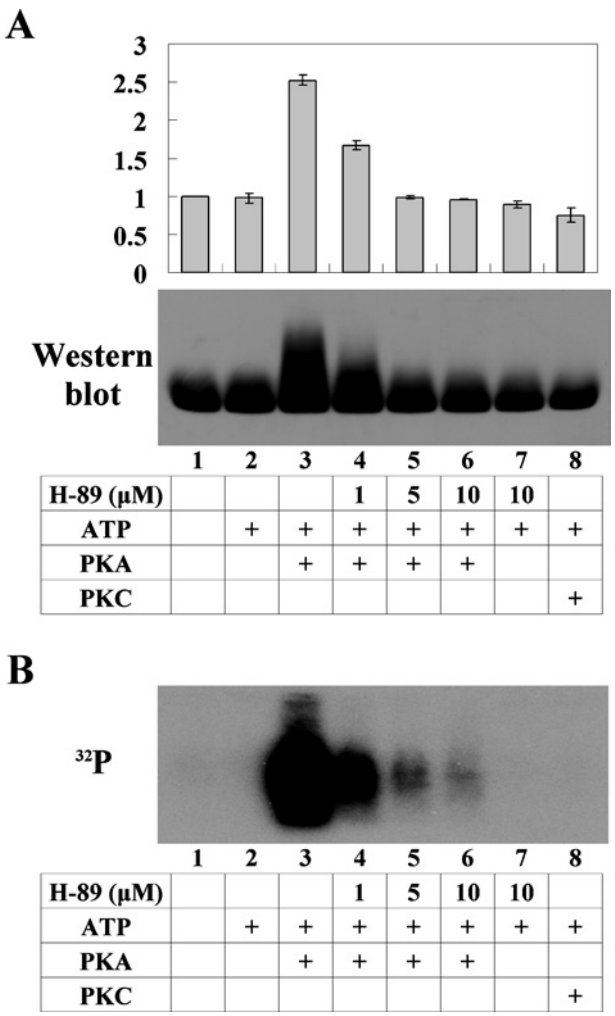

Figure 1 PKA-mediated phosphorylation facilitated HBV core assembly

(**A**) For the *in vitro* kinase assay, 1 unit of PKA (lanes 3–6) was used to phosphorylate Cp149 with 10 μM ATP (lanes 2–8). To inhibit the PKA-mediated phosphorylation of Cp149, serially diluted H-89 was added to the reaction mixture (lanes 4–6). PKC (1 unit) was used for the control experiment (lane 8). Reaction mixtures were incubated at 30 °C for 30 min and resolved on 0.9 % agarose gel. Western blotting was performed as described in the Materials and methods section. The intensity of the band in lane 1 was set as the standard. (**B**) To detect the phosphorylation of assembled HBV Cp149, 10 μM of [γ-^{32}P]ATP (lanes 2–8) was used instead of unlabelled ATP. Samples were separated on a 0.9 % agarose gel and exposed to an X-ray film. The band intensities were analysed using ImageMaster 2D Elite software 4.01 (Amersham Pharmacia Biotechnology).

For the control experiment, pRc/CMV (Invitrogen, Carlsbad, CA, U.S.A.), the backbone DNA of pCMV/FLAG–Core(WT) and pCMV/FLAG–Core(S87G) were used. After transfection, the cells were cultured for 2 days and harvested. The assembled HBV Cps in the lysate were separated by sucrose step gradient analysis and detected as described previously [23]; the sucrose step gradient buffer was composed of 10 mM Hepes, pH 7.5.

Tryptic in-gel digestion and MALDI–TOF (matrix-assisted laser-desorption ionization–time-of-flight)-MS

Protein bands were excised from an SDS/15 % PAGE gel and in-gel digestion was performed as described previously [25]. Mass spectra were obtained using the MALDI–TOF-TOF 4700 tandem mass spectrometer (Applied Biosystems, CA, U.S.A.). The peptide digest was mixed with a matrix and the mixture

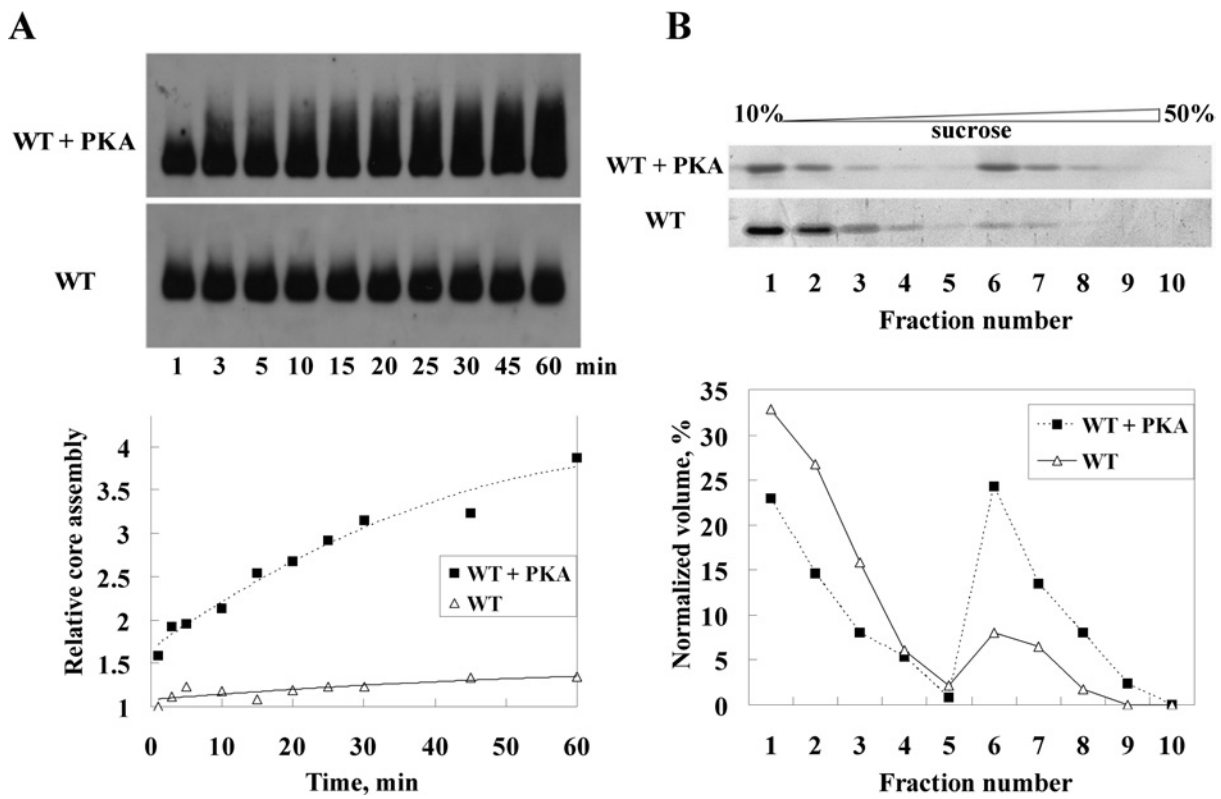

Figure 2 Time course of assembly of WT Cp149

(**A**) The assembled Cp level with (top panel) and without (middle panel) PKA at 30 °C was detected at the designated times by native gel electrophoresis and Western blot analysis. The band intensities were normalized to the intensity of the PKA-untreated Cp149 band at 1 min (middle panel, lane 1); this was set as the standard. The data were fit to a hyperbolic curve. (**B**) Sucrose step gradient analysis (10–50 % sucrose in 10 mM Hepes buffer, pH 7.5) was performed using samples incubated for 1 h. Samples were separated by SDS/PAGE (15 % gel) and visualized using SYPRO Orange (Bio-Rad, Hercules, CA, U.S.A.). Dimeric Cp149 and assembled Cp149 were located at the top (fraction numbers 1–3) and middle (fraction numbers 6 and 7) layers of the sucrose gradient respectively. The intensities of individual bands were analysed using ImageMaster 2D Elite software 4.01 (Amersham Pharmacia Biotechnology) and the calculated level of Cp obtained from PKA-treated Cp149 (■) and Cp149 without treatment (△) are shown (bottom panel).

was applied to a stainless steel plate. To analyse the peptide mass peak, Data Explorer™ software (Applied Biosystems) was used.

RESULTS

Phosphorylation of HBV Cp by PKA facilitates core assembly

To investigate the effect of PKA on HBV core assembly, the assembled Cp level was estimated by native gel electrophoresis and sucrose step gradient analysis, which have been widely used for detecting the capsid form of HBV Cp [26,27].

An *in vitro* kinase assay was performed with and without 1 unit of PKA (Sigma) at 30 °C for 30 min. Samples were separated using native gel electrophoresis to detect the assembled Cp and the phosphorylation of capsid particle. The assembled Cp149 was phosphorylated by PKA (Figure 1B, lane 3). The assembled Cp level in the presence of PKA (Figure 1A, lane 3) increased 2.5-fold compared with the WT Cp without PKA (Figure 1A, lane 2). To determine whether the Cp was specifically phosphorylated by PKA, an *in vitro* kinase assay was carried out using the PKA-specific inhibitor H-89 (Sigma). Cp149 was incubated with serially diluted H-89 (1, 5 or 10 μM) and 1 unit of PKA. The phosphorylation of the assembled Cps was decreased by H-89 (Figure 1B, lanes 4–6) and the level of assembled Cp149 was also reduced (Figure 1A, lanes 4–6). The results show that core phosphorylation and assembly mediated by PKA were inhibited by H-89 in a concentration-dependent manner. On the other hand, PKC neither phosphorylated Cp149 nor affected the assembled Cp level (Figures 1A and B, lanes 8).

To confirm the PKA-mediated increase in HBV core assembly, the time course of the assembled Cp level was assessed. The intensity of the PKA-untreated Cp149 band at 1 min (Figure 2A, middle panel, lane 1) was set as the standard and the relative intensities of the other bands were analysed (Figure 2A, bottom panel). The time course evaluation indicated that the level of assembled PKA-treated WT Cp149 (Figure 2A, top panel) increased at a faster rate compared with that of assembled WT Cp149 without PKA treatment (Figure 2A, middle panel). Sucrose step gradient analysis was also used to confirm the increase in assembled Cp149 by PKA-mediated phosphorylation. The samples were incubated at 30 °C for 1 h without or in the presence of PKA. The samples were fractionated from top to bottom. The dimeric Cp149 and assembled Cp149 were located at the top and middle layers of the sucrose gradient respectively (Figure 2B; fraction number, 1–3 and 6–7 respectively). When PKA was incubated with the reaction mixture, the amount of dimeric Cp149, as indicated by the density of individual bands, was reduced and more assembled Cp149 was formed (Figure 2B). These results show that in contrast to PKC, PKA phosphorylates the N-terminal domain (amino acids 1–149) of the WT Cp and increases the assembled Cp level.

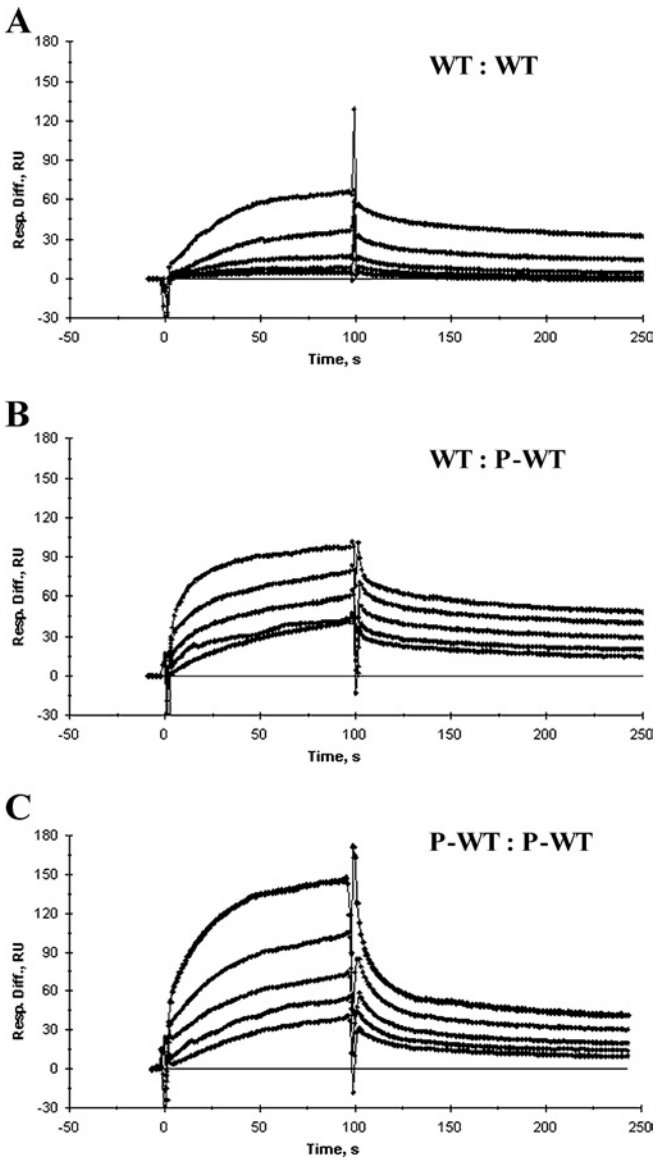

Figure 3 Sensorgrams depicting the binding of PKA-treated (P-WT) and without treatment (WT) Cp149 with immobilized Cp149 using BIAcore 3000

(**A**) WT Cp149 was immobilized on FC2 and WT Cp149 was then injected. (**B**) WT Cp149 was immobilized on FC2 and PKA-phosphorylated WT Cp149 (P-WT) was then injected. (**C**) P-WT Cp149 was immobilized on FC3 and P-WT Cp149 was passed through the flow cell. Five concentrations of Cp149 dimers (10, 5, 2.5, 1.25, and 0.625 μM) were passed through the FC at a flow rate of 60 μl/min. Changes in surface plasmon resonance from experimental flow cells (FC2 and FC3) to first FC (control, without any protein; FC1) were monitored in real time and are shown in the binding curves in response units. Sensorgrams were analysed using the BIAevaluation software version 3.1 (Biacore AB) and the data are shown in Table 1. *1000 RU = change of mass by 1 ng/mm^2.

Comparison of Cp149 protein–protein interactions using the SPR technique

HBV capsid formation starts with the interactions of dimeric Cps. Therefore, to investigate the cause of enhanced *in vitro* core assembly due to PKA, SPR was used to assess the binding affinity between Cp149 dimers. Samples were prepared as described in the Materials and methods section and the analysis was performed using a BIAcore 3000 instrument (Biacore AB). Sensorgrams of the interaction between dimeric Cp149 are shown in Figure 3 and detailed accounts of the kinetics of the interactions between the dimers are listed in Table 1. The association rate constant (k_a) is the rate of formation of a new complex and k_d is the rate of complex dissociation. The values of k_a and k_d fit well to a 1:1 Langmuir binding model while the χ^2 values were generally less than 1.5. The equilibrium dissociation constant (K_D) is defined as k_d/k_a, which represents the affinity between the molecules. The calculated K_D is in the appropriate range that is required for assembly [28]. The K_D of the interaction between WT and PKA-phosphorylated WT (P-WT) Cp149 (9.3×10^{-7}, Table 1, No. 2) was lower than that of the interaction between WT and WT Cp149 (1.3×10^{-5}, Table 1, No. 1). As observed in Table 1 (Nos. 1 and 2), the increase in k_a (10-fold) is the main factor that causes the reduction in K_D (14-fold), whereas no significant decrease in k_d is observed (1.3-fold). This data suggests that the increased affinity between WT Cp149 dimers, as a result of phosphorylation, is mainly due to the elevated rate of dimeric Cp149 association (Figure 3, compare A with B). Furthermore, the K_D of No. 3 (2.6×10^{-7} M) decreased 49-fold when compared with that of No. 1 (1.3×10^{-5} M). This data indicates that dimers combine more rapidly when both the combining Cp dimers are phosphorylated by PKA than when only one of the Cp dimers is phosphorylated. As a result, PKA-mediated phosphorylation may elevate the rate of intermediate formation and the subsequent addition of dimeric Cps, resulting in a marked effect on the rate of capsid formation.

Table 1 Binding parameters obtained from kinetic analysis

Sensorgrams of the interaction between dimeric Cp149 are shown in Figure 3 and the detailed accounts of the kinetics of the interactions and affinities between the dimers are listed here. No. 1 represents the interaction between WT Cp149 and WT Cp149. No. 2 represents the interaction between WT Cp149 and phosphorylated WT Cp149 (P-WT). No. 3 represents the interaction between P-WT Cp149 and P-WT Cp149.

No.	Molecule A	Molecule B	k_a ($M^{-1}s^{-1}$)	k_d (s^{-1})	K_D (M)
1	WT	WT	9.0×10^2	1.1×10^{-2}	1.3×10^{-5}
2	WT	P-WT	9.0×10^3	8.8×10^{-3}	9.3×10^{-7}
3	P-WT	P-WT	1.4×10^4	3.5×10^{-3}	2.6×10^{-7}

Identification of core phosphorylation sites using MALDI–TOF-MS

MALDI–TOF-MS was used to identify the PKA phosphorylation site(s) in Cp149. Cp149 protein expressed in *E. coli* was treated with PKA or untreated. The dimeric WT Cp149 (Figure 4A) and PKA-treated WT Cp149 (Figure 4B) were separated by SDS/PAGE (15% gel) and analysed by MALDI–TOF-MS. The spectrum showed a peak at 1644.7 m/z (Figure 4B) that corresponded to the theoretical m/z of the core peptide comprising 83–96 amino acids (1564.8 m/z) and a single phosphate. There are two possible phosphorylation sites within the core peptide of 83–96 amino acids: Ser^{87} and Tyr^{88}. However, since PKA phosphorylates serine/threonine and the peak did not shift from 1564.8 m/z to 1724.7 m/z (results not shown), which would correspond to two phosphate molecules, Ser^{87} was selected as the putative PKA phosphorylation site.

Comparison of the levels of *in vitro*-assembled WT and mutant Cps

Mutant Cp149 (S87G) was constructed and purified in *E. coli* as described in the Materials and methods section. To study the effect of the S87G mutation on *in vitro* assembly, the assembly reaction was performed with the same amounts (20 μM) of dimeric WT and mutant Cp149. Despite the amino acid change at Ser^{87}, WT and mutant Cp149 revealed almost the same level of core assembly in the absence of PKA *in vitro* (Figure 5, top panel,

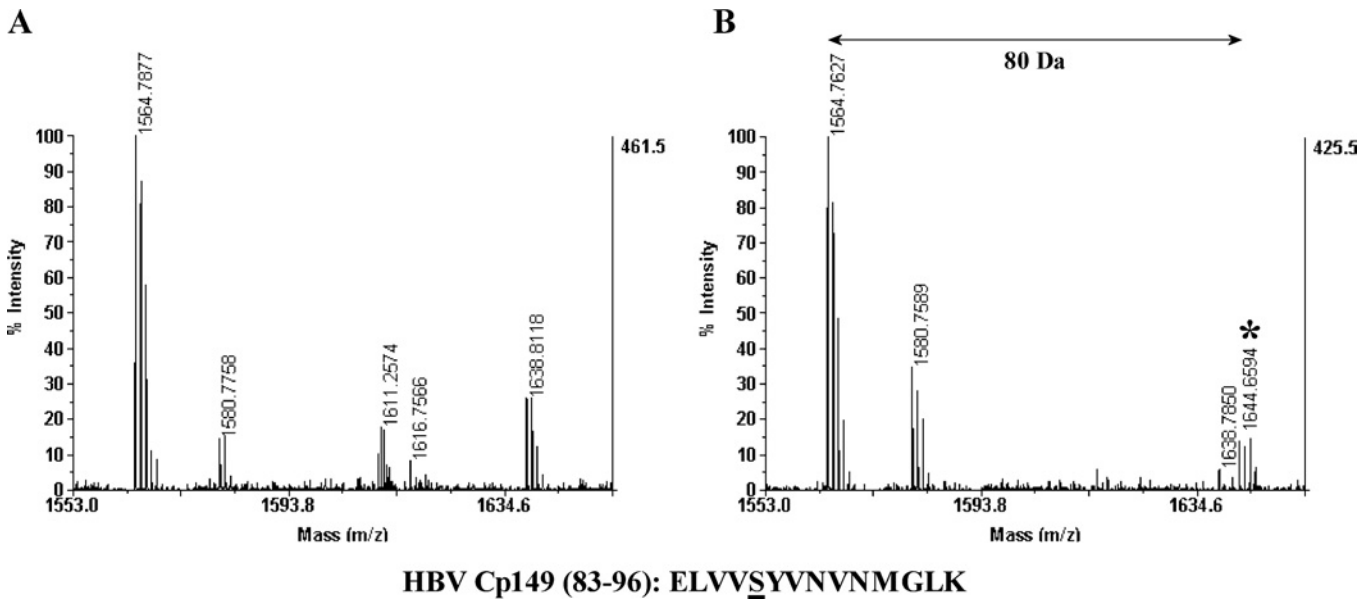

Figure 4 MALDI–TOF-MS was used to detect the PKA phosphorylation site(s)

(**A**) WT Cp149 was purified using the *E. coli* expression system. MALDI–TOF-MS analysis of in-gel digested WT Cp149 dimer was performed. (**B**) PKA-phosphorylated WT Cp149 dimer was analysed to identify the phosphorylation site. The peak at 1564.8 m/z (**A**, **B**) corresponds to that of the HBV core peptide of 83–96 amino acids. One phosphate shifts the original peak (1564.8 m/z) by 80 Da. To analyse the peptide mass peak Data Explorer™ software (Applied Biosystems) was used. * indicates the phosphorylated peptide peak.

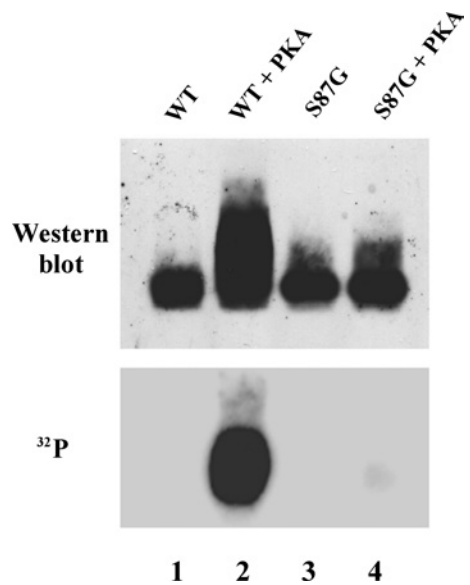

Figure 5 Comparison of the levels of assembled WT with mutant Cps *in vitro*

Same amounts (20 μM) of dimeric WT Cp149 and mutant Cp149 (S87G) were incubated with and without PKA. For the *in vitro* kinase assay, 1 unit of PKA with 10 μM ATP (top panel) and 10 μM of [γ-^{32}P]ATP (bottom panel) were incubated with Cp149 dimers at 30 °C for 30 min. Native gel electrophoresis and Western blot analysis were performed as described in the Materials and methods section.

lanes 1 and 3). When WT and mutant Cp149 were incubated with PKA, the level of assembled WT Cp149 increased (Figure 5, top panel, lane 2), whereas that of assembled mutant Cp149 did not (Figure 5, top panel, lane 4). As shown in Figure 5 bottom panel, the phosphorylation of WT Cp149 (lane 2) was detected using [γ-^{32}P]ATP and the S87G mutation inhibited the phosphorylation of mutant Cp149 (lane 4). This result suggested that Ser^{87} of Cp149 is the unique PKA phosphorylation site, which is in agreement with the result obtained from the MALDI–TOF-MS analysis.

Measurements of assembled Cp149 using TEM (transmission electron microscopy)

To identify whether phosphorylation and mutation of Cp149 affect capsid formation, the *in vitro* assembled core particles were negatively stained and observed by TEM. The diameter of WT Cp149 was determined to be approximately 30 nm ($T = 4$ form) [29]. From the TEM data, the approximate diameters of the WT Cp149 capsid (Figure 6A) and the PKA-treated core particle (Figure 6B) were estimated to be 30 nm (average diameters of 30.27 and 30.38 nm respectively). In addition, the approximate diameter of mutant Cp149 (S87G) (Figure 6C) was also estimated to be 30 nm (with an average diameter of 30.25 nm). The shapes of these *in vitro* assembled Cps were also identical (Figure 6A, B and C). From these results, the PKA-treated WT core particles and mutant core particles were considered to be identical with the WT Cp149 particles with regard to their morphology.

Comparison of the core assembly between WT and mutant Cps in HepG2 cells

To identify the effect of phosphorylation on *in vivo* core assembly, FLAG- tagged WT and mutant (S87G) Cps were transfected into HepG2 cells. Cell lysates from each sample were resolved by SDS/PAGE (15 % gels) and Western blot analysis with anti-FLAG antibody (Sigma) was performed to detect the total expressed Cp. The assembled Cps in HepG2 cells were separated by native agarose gel electrophoresis, and Western blot analysis with anti-HBc antibody was carried out for their detection. The results of the Western blots were quantified as described previously [23]. The amount of WT capsid protein (Figure 7, middle panel, lane 2)

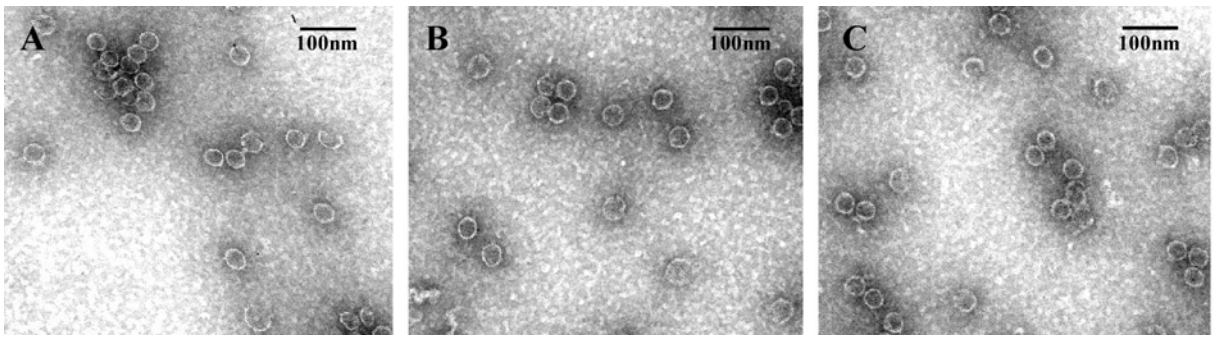

Figure 6 Electron micrographs of assembled core particles

Assembled core particles were negatively stained with 2% uranyl acetate. (**A**) Dimeric WT Cp149 was assembled in a reaction buffer (10 mM Hepes, pH 7.5 and 10 mM $MgCl_2$). (**B**) Dimeric WT Cp149 was assembled with PKA in a reaction buffer containing 10 μM ATP. (**C**) Dimeric mutant Cp149 (S87G) was assembled in a reaction buffer. Scale bar = 100 nm.

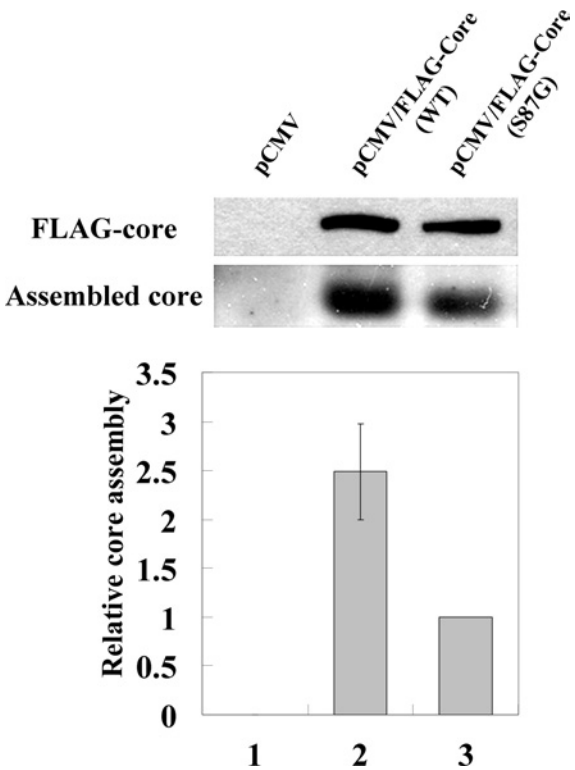

Figure 7 Comparison of WT and mutant Cps in HepG2 cells

To detect cytoplasmic HBV Cp, the HepG2 cells were transfected with pCMV/FLAG–Core(WT) (lane 2) and pCMV/FLAG–Core(S87G) (lane 3). Backbone DNA (pRc/CMV) was transfected as a control (lane 1). Total Cps were separated by SDS/PAGE (15% gel; top panel) and detected by Western blotting with anti-FLAG antibody. The assembled Cps were separated on 0.9% native agarose gel (middle panel) and detected by Western blotting with anti-HBc antibody. The band intensities were normalized to the intensity of the pCMV/FLAG–Core(S87G) band, which was set as the standard (bottom panel).

increased 2.5-fold in comparison with the mutant capsid protein (Figure 7, middle panel, lane 3), although the same level of total Cp was expressed in both cases (Figure 7, top panel, lanes 2 and 3). The backbone DNA that was used as a control did not express Cp in HepG2 cells (Figure 7, top panel, lane 1). These results suggest that the phosphorylation of Cp at Ser^{87} elevated the level of *in vivo* core assembly.

DISCUSSION

The regulation of pgRNA encapsidation and viral replication by several kinases has been investigated mainly through the phosphorylation of the C-terminal domain of HBV Cp. However, in the present report, we have investigated the PKA-mediated phosphorylation of the N-terminal domain of the HBV Cp and the increased HBV core assembly by *in vitro* phosphorylation. SPR was used to investigate the factors that cause increased core assembly, which revealed that increased core assembly was due mainly to the elevated rate of dimeric Cp149 association as a result of PKA-mediated phosphorylation. Using MALDI–TOF-MS, Ser^{87} of the Cp was identified as the specific PKA phosphorylation site, and the PKA-mediated increase in core assembly was inhibited by replacing Ser^{87} with glycine *in vitro*. When WT and mutant (S87G) genes were transfected into HepG2 cells, the mutant Cp also showed a lower assembly compared with the WT Cp.

Ser^{87} is present in the fourth α-helix structure of the Cp, which is far from important residues (namely, amino acids 113–143) involved in the interactions between dimers [30]. However, previous reports have indicated that core assembly is facilitated by naturally occurring F97L mutation in the fourth α-helix of HBV Cp [13], and that cations such as Zn^{2+}, Ca^{2+} and Na^{+} also facilitate core assembly [24,28,31] by altering protein conformation. It has been shown that PKA causes conformational changes in proteins [32]. Therefore the increase in HBV core assembly may be due to the conformational change induced by PKA-mediated phosphorylation of HBV Cp at Ser^{87}.

In the early stages of viral infection, a high level of serum HBV DNA is detected [33]. Subsequently, patients enter the chronic phase that is accompanied by changes in the amino acids of the immunological epitope of the HBV Cp due to immune pressure; the patients show decreased serum HBV DNA level [33–35]. The fourth α-helix structure of the Cp is an immunological epitope for B and T cells, which is highly mutated in chronic HBV-infected patients. Ser^{87} is also mutated in the chronic phase and is predominantly substituted with glycine [33,35–38]. Our results suggest that the *in vitro* PKA-mediated phosphorylation of HBV Cp at Ser^{87} facilitated core assembly. However, S87G mutation inhibited the PKA-mediated phosphorylation of the HBV Cp and caused reduction in the assembled Cp level. Since HBV core assembly is followed by viral replication, S87G mutation may cause a decrease in the serum HBV DNA level in the chronic phase through impaired core assembly.

In HBV core assembly, a trimer of dimeric Cp nucleates capsid assembly and at least 0.7–0.8 μM of dimeric Cp is

required for capsid formation [8,39]. Using SPR, the association value of PKA-phosphorylated Cp149 dimers was estimated to be approx. 40 RU, whereas that of unphosphorylated Cp149 dimers was less than 6 RU. This was observed at a dimeric Cp149 concentration of 0.625 μM, which is lower than that required for core assembly. This data supported the fact that increased affinity of phosphorylated dimers may facilitate the formation of the core nucleus, although the concentration of HBV Cp may not be sufficient for capsid assembly.

On the basis of the results of this study, we suggest that PKA is a new factor that facilitates the HBV core assembly via the phosphorylation of the HBV Cp. The PKA-mediated phosphorylation of the dimeric Cp at Ser^{87} increases the affinity between Cp dimers and facilitates HBV core assembly both *in vitro* and *in vivo*. Since HBV core assembly is followed by viral replication, our results will be useful in understanding the regulation of viral replication through the phosphorylation of the HBV Cp.

This work was supported by Korean Research Foundation Grant (KRF-2003-015-C00490). H.Y.K. and S.L. are supported by the BK21 Research Fellowship from the Ministry of Education and Human Resource Development.

REFERENCES

1 Vanlandschoot, P., Cao, T. and Leroux-Roels, G. (2003) The nucleocapsid of the hepatitis B virus: a remarkable immunogenic structure. Antiviral. Res. **60**, 67–74
2 Beasley, R. P., Hwang, L. Y., Lin, C. C. and Chien, C. S. (1981) Hepatocellular carcinoma and hepatitis B virus. A prospective study of 22 707 men in Taiwan. Lancet **2**, 1129–1133
3 Kidd-Ljunggren, K., Oberg, M. and Kidd, A. H. (1995) The hepatitis B virus X gene: analysis of functional domain variation and gene phylogeny using multiple sequences. J. Gen. Virol. **76**, 2119–2130
4 Kao, J. H., Chen, P. J., Lai, M. Y. and Chen, D. S. (2000) Hepatitis B genotypes correlate with clinical outcomes in patients with chronic hepatitis B. Gastroenterology **118**, 554–559
5 Sugauchi, F., Ohno, T., Orito, E., Sakugawa, H., Ichida, T., Komatsu, M., Kuramitsu, T., Ueda, R., Miyakawa, Y. and Mizokami, M. (2003) Influence of hepatitis B virus genotypes on the development of preS deletions and advanced liver disease. J. Med. Virol. **70**, 537–544
6 Tiollais, P., Pourcel, C. and Dejean, A. (1985) The hepatitis B virus. Nature (London) **317**, 489–495
7 Nassal, M. and Schaller, H. (1996) Hepatitis B virus replication – an update. J. Viral. Hepat. **3**, 217–226
8 Zlotnick, A., Johnson, J. M., Wingfield, P. W., Stahl, S. J. and Endres, D. (1999) A theoretical model successfully identifies features of hepatitis B virus capsid assembly. Biochemistry **38**, 14644–14652
9 Watts, N. R., Conway, J. F., Cheng, N., Stahl, S. J., Belnap, D. M., Steven, A. C. and Wingfield, P. T. (2002) The morphogenic linker peptide of HBV capsid protein forms a mobile array on the interior surface. EMBO J. **21**, 876–884
10 Zlotnick, A., Cheng, N., Conway, J. F., Booy, F. P., Steven, A. C., Stahl, S. J. and Wingfield, P. T. (1996) Dimorphism of hepatitis B virus capsids is strongly influenced by the C-terminus of the capsid protein. Biochemistry **35**, 7412–7421
11 Cohen, B. J. and Richmond, J. E. (1982) Electron microscopy of hepatitis B core antigen synthesized in *E. coli*. Nature (London) **296**, 677–679
12 Stahl, S., MacKay, P., Magazin, M., Bruce, S. A. and Murray, K. (1982) Hepatitis B virus core antigen: synthesis in *Escherichia coli* and application in diagnosis. Proc. Natl. Acad. Sci. U.S.A. **79**, 1606–1610
13 Ceres, P., Stray, S. J. and Zlotnick, A. (2004) Hepatitis B virus capsid assembly is enhanced by naturally occurring mutation F97L. J. Virol. **78**, 9538–9543
14 Lan, Y. T., Li, J., Liao, W. and Ou, J. (1999) Roles of the three major phosphorylation sites of hepatitis B virus Cp in viral replication. Virology **259**, 342–348
15 Nassal, M. (1992) The arginine-rich domain of the hepatitis B virus Cp is required for pregenome encapsidation and productive viral positive-strand DNA synthesis but not for virus assembly. J. Virol. **66**, 4107–4116
16 Kann, M. and Gerlich, W. H. (1994) Effect of Cp phosphorylation by protein kinase C on encapsidation of RNA within core particles of hepatitis B virus. J. Virol. **68**, 7993–8000
17 Kau, J. H. and Ting, L. P. (1998) Phosphorylation of the Cp of hepatitis B virus by a 46-kilodalton serine kinase. J. Virol. **72**, 3796–3803
18 Liao, W. and Ou, J. H. (1995) Phosphorylation and nuclear localization of the hepatitis B virus Cp: significance of serine in the three repeated SPRRR motifs. J. Virol. **69**, 1025–1029
19 Daub, H., Blencke, S., Habenberger, P., Kurtenbach, A., Dennenmoser, J., Wissing, J., Ullrich, A. and Cotten, M. (2002) Identification of SRPK1 and SRPK2 as the major cellular protein kinases phosphorylating hepatitis B virus Cp. J. Virol. **76**, 8124–8137
20 Yu, M. and Summers, J. (1994) Phosphorylation of the duck hepatitis B virus capsid protein associated with conformational changes in the C terminus. J. Virol. **68**, 2965–2969
21 Kann, M., Sodeik, B., Vlachou, A., Gerlich, W. H. and Helenius, A. (1999) Phosphorylation-dependent binding of hepatitis B virus core particles to the nuclear pore complex. J. Cell. Biol. **145**, 45–55
22 Barrasa, M. I., Guo, J. T., Saputelli, J., Mason, W. S. and Seeger, C. (2001) Does a cdc2 kinase-like recognition motif on the Cp of hepadnaviruses regulate assembly and disintegration of capsids? J. Virol. **75**, 2024–2028
23 Park, S. G., Lee, S. M. and Jung, G. (2003) Antisense oligodeoxynucleotides targeted against molecular chaperonin Hsp60 block human hepatitis B virus replication. J. Biol. Chem. **278**, 39851–39857
24 Choi, Y., Gyoo Park, S., Yoo, J. H. and Jung, G. (2005) Calcium ions affect the hepatitis B virus core assembly. Virology **332**, 454–463
25 Kim, W., Oe Lim, S., Kim, J. S., Ryu, Y. H., Byeon, J. Y., Kim, H. J., Kim, Y. I., Heo, J. S., Park, Y. M. and Jung, G. (2003) Comparison of proteome between hepatitis B virus- and hepatitis C virus-associated hepatocellular carcinoma. Clin. Cancer Res. **9**, 5493–5500
26 Konig, S., Beterams, G. and Nassal, M. (1998) Mapping of homologous interaction sites in the hepatitis B virus Cp. J. Virol. **72**, 4997–5005
27 Koschel, M., Thomssen, R. and Bruss, V. (1999) Extensive mutagenesis of the hepatitis B virus core gene and mapping of mutations that allow capsid formation. J. Virol. **73**, 2153–2160
28 Ceres, P. and Zlotnick, A. (2002) Weak protein-protein interactions are sufficient to drive assembly of hepatitis B virus capsids. Biochemistry **41**, 11525–11531
29 Newman, M., Suk, F. M., Cajimat, M., Chua, P. K. and Shih, C. (2003) Stability and morphology comparisons of self-assembled virus-like particles from wild-type and mutant human hepatitis B virus capsid proteins. J. Virol. **77**, 12950–12960
30 Pumpens, P. and Grens, E. (1999) Hepatitis B core particles as a universal display model: a structure-function basis for development. FEBS Lett. **442**, 1–6
31 Stray, S. J., Ceres, P. and Zlotnick, A. (2004) Zinc ions trigger conformational change and oligomerization of hepatitis B virus capsid protein. Biochemistry **43**, 9989–9998
32 Grimard, V., Li, C., Ramjeesingh, M., Bear, C. E., Goormaghtigh, E. and Ruysschaert, J. M. (2004) Phosphorylation-induced conformational changes of cystic fibrosis transmembrane conductance regulator monitored by attenuated total reflection-Fourier transform IR spectroscopy and fluorescence spectroscopy. J. Biol. Chem. **279**, 5528–5536
33 Bozkaya, H., Ayola, B. and Lok, A. S. (1996) High rate of mutations in the hepatitis B core gene during the immune clearance phase of chronic hepatitis B virus infection. Hepatology **24**, 32–37
34 Akarca, U. S. and Lok, A. S. (1995) Naturally occurring hepatitis B virus core gene mutations. Hepatology **22**, 50–60
35 Hosono, S., Tai, P. C., Wang, W., Ambrose, M., Hwang, D. G., Yuan, T. T., Peng, B. H., Yang, C. S., Lee, C. S. and Shih, C. (1995) Core antigen mutations of human hepatitis B virus in hepatomas accumulate in MHC class II-restricted T cell epitopes. Virology **212**, 151–162
36 Ehata, T., Omata, M., Yokosuka, O., Hosoda, K. and Ohto, M. (1992) Variations in codons 84–101 in the core nucleotide sequence correlate with hepatocellular injury in chronic hepatitis B virus infection. J. Clin. Invest. **89**, 332–338
37 Chuang, W. L., Omata, M., Ehata, T., Yokosuka, O., Ito, Y., Imazeki, F., Lu, S. N., Chang, W. Y. and Ohto, M. (1993) Precore mutations and core clustering mutations in chronic hepatitis B virus infection. Gastroenterology **104**, 263–271
38 Ni, Y. H., Chang, M. H., Hsu, H. Y. and Tsuei, D. J. (2003) Different hepatitis B virus core gene mutations in children with chronic infection and hepatocellular carcinoma. Gut **52**, 122–125
39 Seifer, M., Zhou, S. and Standring, D. N. (1993) A micromolar pool of antigenically distinct precursors is required to initiate cooperative assembly of hepatitis B virus capsids in *Xenopus* oocytes. J. Virol. **67**, 249–257

Received 2 March 2006/31 May 2006; accepted 2 June 2006
Published as BJ Immediate Publication 2 June 2006, doi:10.1042/BJ20060347